CHINESE GEOGRAPHICAL SCIENCE
Volume 16, Number 2, pp. 171-175, 2006
Science Press, Beijing, China

NORMALIZED DIFFERENCE SNOW INDEX SIMULATION FOR SNOW-COVER MAPPING IN FOREST BY GEOSAIL MODEL

CAO Yun-gang[1,2], LIU Chuang[1]
(1. Institute of Geographical Sciences and Natural Resources Research, Chinese Academy of Sciences, Beijing 100101, P.R. China; 2. Graduate School of Chinese Academy of Sciences, Beijing 100049, P. R. China)

ABSTRACT: The snow-cover mapping in forest area is always one of the difficult points for optical satellite remote sensing. To investigate reflectance variability and to improve the mapping of snow in forest area, GeoSail model was used to simulate the reflectance of a snow-covered forest. Using this model, the effects of varying canopy density, solar illumination and view geometry on the performance of the MODIS (Moderate-resolution Imaging Spectroradiometer) snow-cover mapping algorithm were investigated. The relationship between NDSI (Normalized Difference Snow Index), NDVI (Normalized Difference Vegetation Index) and snow fraction was discussed in detail. Results indicated that the weak performance would be achieved if fixed criteria were used for different regions especially in the complicated land cover components. Finally, some suggestions to MODIS SNOWMAP algorithm were put forward to improve snow mapping precision in forest area based on the simulation, for example, new criteria should be used in coniferous forest, that is, NDSI greater than 0.3 and NDVI greater than zero. Otherwise, a threshold on view zenith angle may be used in the criteria such as 45°.
KEY WORDS: snow cover mapping; reflectance model; MODIS

CLC number: TP753 Document code: A Article ID: 1002-0063(2006)02-0171-05

1 INTRODUCTION

Snow is an important component of the Earth's surface. Up to $50\times10^6 km^2$ (34%) of the Earth's land surface is seasonally snow-covered (VIKHAMAR and SOLBERG, 2002). Compared to other land covers, snow cover extent varies dramatically on very short time scales (hours-months). Its presence affects physical, chemical and biological processes at many spatial scales and has important social impacts. At the global scale, its high albedo strongly influences the Earth's radiation budget (KLEIN et al., 1998). So changes in the amount and extent of snow cover may accompany global climate change.

Monitoring of global snow cover is possible with satellite-borne sensors that observe the Earth's surface. Satellite remote sensing is a useful tool for monitoring the snow cover because it enables observations of large and remote areas. Satellite images from optical and microwave sensors are available in different temporal, spatial and spectral resolutions. Although microwave sensors have received much attention in the related researches over the last decades, methods based on optical images currently provide the most accurate snow-cover area estimate for cloud-free situations (SOLBERG et al., 1997). Optical sensors can distinguish between snow-covered and snow-free grounds. This is based on the very high reflectance of snow in visible wavelengths compared with other natural targets. Snow-cover mapping methods for optical images include unsupervised and supervised classification algorithms, spectral mixture analysis, the MODIS snow-mapping algorithm, etc. (VIKHAMAR and SOLBERG, 2003; HALL et al., 1995). Specially, the MODIS snow-mapping algorithm uses criteria tests to identify snow-covered pixels, where the Normalized Difference Snow Index (NDSI) constitutes an important element. This algorithm is simple, effective and exercisable. The relative accuracy of the algorithm is estimated to be 99% in non-forest areas and 85% in forest areas with full snow coverage (HALL et al., 2001). Traditionally, forests are considered a problem in snow mapping. Trees increase the complexity of the scene: on one hand, they reduce the signal from ground to the satellite sensor, and on the other hand, they contribute to the observed reflectance. As a consequence,

Received date: 2005-12-08
Biography: CAO Yun-gang (1978-), male, a native of Chengdu of Sichuan Province, Ph.D. candidate, specialized in remote sensing modeling and application. E-mail: yungang78@163.com

snow is mapped with lower accuracy in forest areas than in non-forest areas (SARI et al., 2005).

To improve the ability of snow cover mapping in forest area, the details of interaction between canopies and photons must be known. In the past two decades, many scientists have simulated the reflectance using different models in forest. Generally, the forests are dynamic and under constant disturbance and recovery cycle, which leads to a strong fragmentation and multilayered vegetation. Relatively few tree species dominate the forests, but the understorey vegetation is very heterogeneous, depending on the soil type and the stand age (SARI et al., 2005). In fact, full forest information on earth surface is not available. Furthermore, the model will be more complicated and unstable if too many factors are taken into account. Fortunately, a convenient model—GeoSail model has been used successfully in analysis of boreal forest landscapes. So the reflectance of a snow-covered forest stand may be simulated using this model.

2 METHOD

In forest, the reflectance of the stand can be modeled as a linear combination of four elements and their areal proportions:

$$\rho=A_{C_{sun}}\rho_{C_{sun}}+A_{C_{shadow}}\rho_{C_{shadow}}+A_{B_{sun}}\rho_{B_{sun}}+A_{B_{shadow}}\rho_{B_{shadow}} \quad (1)$$

where ρ is the total reflectance, $\rho_{C_{sun}}$, $\rho_{C_{shadow}}$, $\rho_{B_{sun}}$, $\rho_{B_{shadow}}$ are the reflectances of sunlit crown, shadowed crown, sunlit background and shadowed background, respectively, and $A_{C_{sun}}$, $A_{C_{shadow}}$, $A_{B_{sun}}$, $A_{B_{shadow}}$ are the areal proportions of four components (WOODCOCK et al., 1997; LI and STRAHLER, 1986).

In snow-covered forest, reflectance of a scene can be calculated:

$$\rho=A_{C_{sun}}\rho_{C_{sun}}+A_{C_{shadow}}\rho_{C_{shadow}}+A_{B_{sun}}\rho_{B_{sun}}+A_{B_{shadow}}\rho_{B_{shadow}}+A_{S_{sun}}\rho_{S_{sun}}+A_{S_{shadow}}\rho_{S_{shadow}} \quad (2)$$

where $\rho_{S_{sun}}$, $\rho_{S_{shadow}}$ are the reflectances of sunlit snow and shadowed snow, $A_{S_{sun}}$, $A_{S_{shadow}}$ are their areal proportions.

In this paper, we used GeoSail model to simulate the reflectance of forest. The GeoSail model combines a geometric model—Jasinski model (JASINSKI and EAGLESON, 1989; 1990) that calculates the amount of shadowed and illuminated components in a scene with a turbid media model—Sail model (VERHOEF, 1984) that calculates the reflectance and transmittance of the tree crowns. It is designed to use canopy component optical properties, tree shape, solar zenith angle, and canopy cover to calculate scene reflectance and the fraction of absorbed photosynthetically active radiation (FAPAR) or fraction of intercepted photosynthetically active radiation (FIPAR) for forest stands (HUEMMRICH, 2001). The Sail model provides the within-tree radiative transfer calculations and Jasinski model combines the Sail results into a scene reflectance. GeoSail makes several assumptions, which allow the model to be computationally simple, yet provides reasonable descriptions of forest canopy reflectance. In GeoSail, all trees have the same shape and size; trees do not shadow each other; tree crowns do not overlap each other; the size of the tree is small compared to the size of the pixel; the illuminated canopy, illuminated background, and shadows each has a single reflectance.

The Jasinski model consists of a scene made up of geometric solids scattered over a plane with a Poisson distribution. Then the fraction of a scene that is shadowed is determined by

$$A_{T_{shadow}}=1-A_{C_{total}}-(1-A_{C_{total}})^{\eta+1} \quad (3)$$

where $A_{T_{shadow}}$ is the total fraction of shadowed area ($A_{S_{shadow}}+A_{B_{shadow}}$) and $A_{C_{total}}$ is the fraction covered by the canopy coverage ($A_{C_{sun}}+A_{C_{shadow}}$). The parameter η is the ratio of canopy cover to shadow area for a single crown. To conifers in winter, canopy components are assumed to be cones solids. Then η is calculated as below:

$$\alpha=\arctan(\frac{r}{h}) \quad (4)$$

$$\beta=\arccos(\frac{\tan\alpha}{\tan\theta}) \quad (5)$$

$$\eta=(\tan\beta-\beta)/\pi \quad (6)$$

For cones, $A_{C_{shadow}}$ is:

$$A_{C_{shadow}}=\frac{\beta}{\pi} \quad (7)$$

where r is the radius of tree canopy. h is the height of the tree. β is determined by the aspect angle of the cone (α) and the solar zenith angle (θ).

Illuminated areal proportions ($A_{S_{sun}}+B_{S_{sun}}$) can then be calculated based on the fractions of $A_{C_{total}}$ and $A_{T_{shadow}}$.

$$A_{T_{sun}}=1-A_{C_{total}}-A_{T_{shadow}} \quad (8)$$

3 RESULTS AND DISCUSSION

In this study, the source code of Sail model wrote by Huemmrich was compiled and reflectance of each component was calculated with this program. The areal proportion of each component was calculated with Jasinski model. We assumed that the snow fraction was a constant and set to 0.5. With this assumption, the proportions of snow and background in each case (sunlit or shadowed) were defined as 0.5:(0.5-$A_{C_{total}}$). Some parameters used in the GeoSail model are listed in Table 1.

The reflectance, NDSI and NDVI were calculated us-

Table 1 Spectral parameters of each component

Wavelength (μm)	Canopy reflectance	Canopy transmittance	Twig reflectance	Background reflectance	Snow reflectance
0.550	0.1405	0.0644	0.204	0.1284	0.9211
0.645	0.0974	0.0221	0.245	0.1495	0.8965
0.858	0.4685	0.3857	0.486	0.2393	0.7869
1.640	0.2562	0.1777	0.285	0.3187	0.055

Notes: (1) Tree species: Pinus banksiana (cone crown); (2) $\frac{r}{h}$: 7.0, LAI: 4.0, twigs: 15%, leaves: 85%; (3) Spherical and planophile leaf angle distributions are used for leaves and twigs, respectively; (4) Background: soil with leaf litter and snow cover

ing GeoSail model with the input list in Table 1. The relationships between NDSI, NDVI and snow fraction, imaging geometry were discussed below.

3.1 NDSI and View Zenith Angle

In general, NDSI decreases as view zenith angle increases. At a lower view zenith angle, the difference of NDSI in three canopy densities is very small. But NDSI decreases quickly at high view zenith angle. On the other hand, the speed of the decrease in principal plane is different for variational direction. For example, the variation of NDSI at negative direction is greater than that at positive direction (Fig. 1).

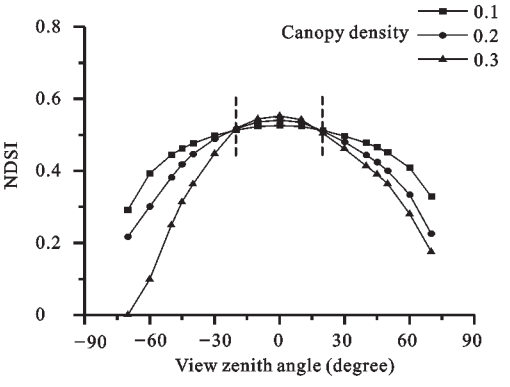

Solar zenith angle is 45 ° and snow fraction is 0.5
Fig. 1 View zenith angle versus NDSI plot for Pinus banksiana

3.2 NDSI and Solar Zenith Angle

The NDSI decreases as solar zenith angle increases. In different canopy densities, the effects are different. At a small solar zenith angle (<50 °), the influence of the solar zenith angle on NDSI is very slight. In this range, NDSI increases as canopy density increases. But NDSI decreases quickly as angle exceed 50 °. In fact, the higher the canopy density, the larger solar zenith angle, and the more variations in NDSI are due to the increase of shadowed area (Fig. 2).

3.3 NDSI and Snow Fraction

Snow fraction is defined as snow-cover areal percentage

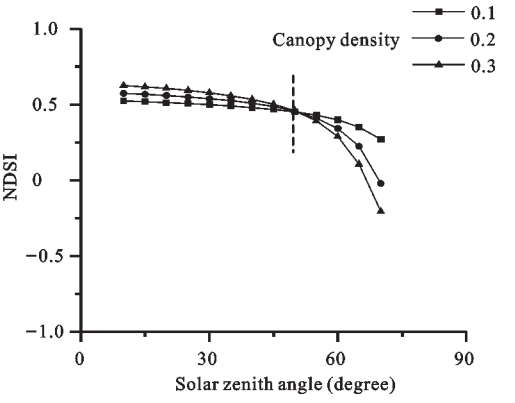

View zenith angle is 0 ° and snow fraction is 0.5
Fig. 2 Solar zenith angle versus NDSI plot for Pinus banksiana

within one pixel. As snow fraction is very high or NDSI is big, the correlation coefficient between them is very high. The correlation of them becomes weaker when snow fraction decreases. NDSI varies slowly in the scene with high vegetation cover, but quickly in the scene with little vegetation (especially bare ground). As a result, we can use quadratic to describe the relationship between NDSI and snow fraction in forest and use a linear model in low vegetation cover area (Fig. 3).

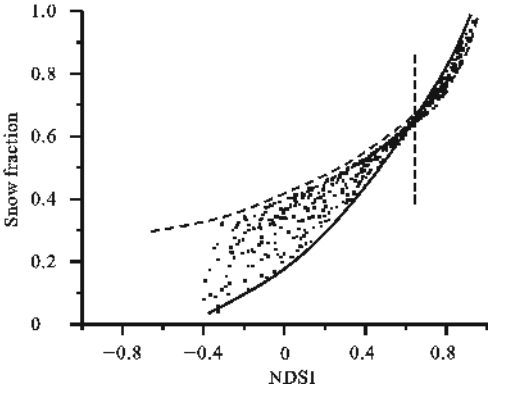

Solar zenith angle is 45 ° and view zenith angle is 0 °
Fig. 3 NDSI versus snow fraction plot for Pinus banksiana

3.4 NDVI and Snow Fraction

There is low correlation between NDVI and snow fraction (Fig. 4). In bare ground, NDVI varies little when snow fraction decreases. Only in forest, NDVI varies from - 0.1 to 0.4 (i.e. canopy density increases). Here, many snow covered speckles are under the shadow of the canopy, so snow fraction observed decreases.

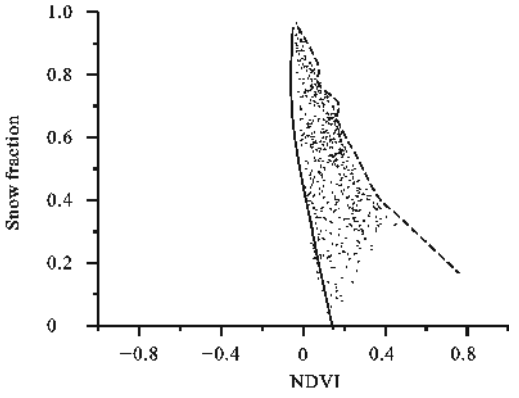

Solar zenith angle is 45 ° and view zenith angle is 0 °
Fig. 4 NDVI versus snow fraction plot for Pinus banksiana

3.5 NDSI, NDVI and Snow Fraction

According to Fig. 5, the NDSI is less than 0.4 although snow fraction is greater than 0.5. As we know, the criterion for MODIS snow-cover mapping is that the pixel is snow-covered when NDSI is greater than 0.4. With this criterion, snow-covered pixels will be underestimated in coniferous forest areas. In our simulation, almost 30% snow-covered pixels are not marked.

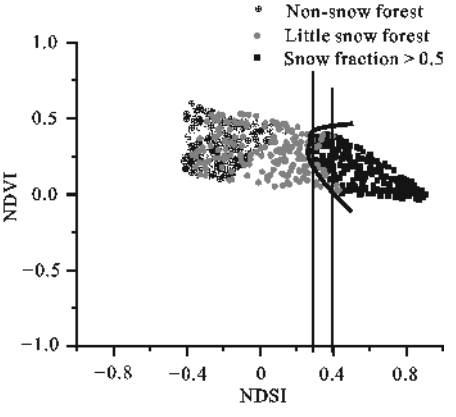

Solar zenith angle is 45 ° and view zenith angle is 0 °
Fig. 5 NDSI versus NDVI plot for Pinus banksiana

In summary, the relationship between snow fraction and NDSI could become weak as the vegetation cover is complicated or imaging geometry is not adaptive. So other information must be used to identify snow-covered area together with NDSI. To improve the snow-cover mapping precision, diverse criteria are also required for different situations. One case is that new criteria should be used in coniferous forest, such as NDSI great than 0.3 and NDVI great than zero. Otherwise, a threshold on view zenith angle may be used in the criteria such as 45 °.

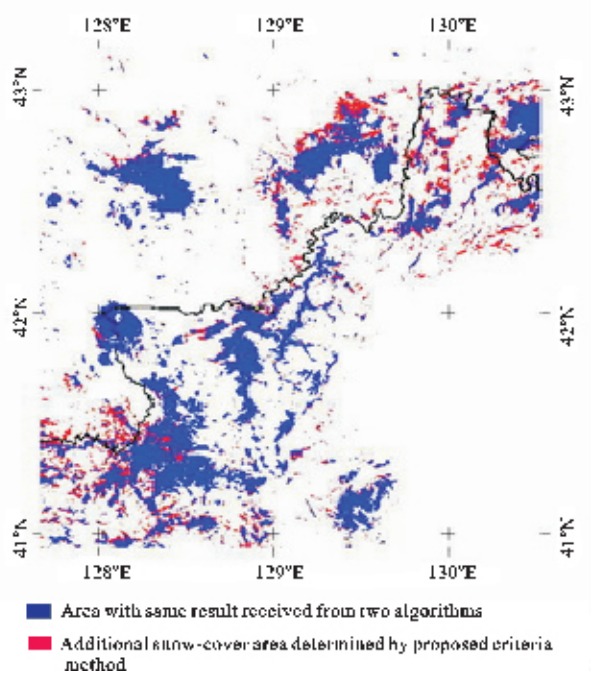

Fig. 6 Snow-cover map difference between MODIS algorithm and proposed criteria method (2005-11-30)

Difference of snow-cover maps between MODIS algorithm and the proposed algorithm of this paper was shown in Fig. 6 (a case study in the Changbai Mountains, Jilin Province). The blue showed the region that the same result received from two algorithms. The red indicated the additional snow cover areas determined by the proposed method. The additional areas are thick coniferous forest according to China Vegetation Cover Map with 1km resolution. The result indicated that the proposed method could identify more snow-cover pixels than MODIS snow-cover mapping algorithm.

4 CONCLUSIONS

The objective of this study is to find out the weakness of MODIS snow-cover mapping algorithm in forest area and propose a new method to improve it. To a snow-cover mapping algorithm just like MODIS snow-cover mapping algorithm, the criteria are very important, but it is

not universal to the regions all over the world. There are many factors that affect criteria such as land cover type, solar zenith angle, view zenith angle, snow grain size and geomorphy, etc. In this study, we use GeoSail model to simulate the reflectance and NDSI, NDVI for a scene in various conditions. The results indicate that correlation coefficient between NDSI and snow fraction is very high while snow fraction is high. However, vegetation cover, solar zenith angle and view zenith angle have more impact on the value of NDSI while snow fraction is low. We change the criteria by analyzing the results. For coniferous forest area, the criteria are NDSI that is greater than 0.3 and NDVI that is greater than 0.1. A threshold on view zenith angle is also used. In addition, suggestions of this study may be only suitable for coniferous forest. Other study should be done for different conditions later. Foremost, validation must be performed for these criteria widely.

REFERENCES

HALL Dorothy K, RIGGS George A, SALOMONSON Vincent V, 1995. Development of methods for mapping global snow cover using Moderate Resolution Imaging Spectroradiometer data [J]. Remote Sensing of Environment, 54: 127- 140.

HALL Dorothy K, FOSTER James L, SALOMONSON Vincent V, 2001. Development of a technique to assess snow-cover mapping errors from space [J]. IEEE Transactions on Geoscience and Remote Sensing, 39 (2): 432- 438.

HUEMMRICH K F, 2001. The GeoSail model: a simple addition to the Sail model to describe discontinuous canopy reflectance [J]. Remote Sensing of Environment, 75: 423- 431.

JASINSKI Michael F, EAGLESON Peter S, 1989. The structure of red-infrared scattergrams of semivegetated landscapes [J]. IEEE Transactions on Geoscience and Remote Sensing, 27 (4): 441- 451.

JASINSKI Michael F, EAGLESON Peter S, 1990. Estimation of subpixel vegetation cover using red-infrared scattergrams [J]. IEEE Transactions on Geoscience and Remote Sensing, 28 (2): 253- 267.

KLEIN Andrew G, HALL Dorothy K, RIGGS George A, 1998. Improving snow-cover mapping in forests through the use of a canopy reflectance model [J]. Hydrological Processes, 12: 1723- 1744.

LI Xiaowen, STRAHLER Alan H, 1986. Geometric-optical bidirectional reflectance modeling of a conifer forest canopy [J]. IEEE Transactions on Geoscience and Remote Sensing, 24: 906- 919.

SARI J Metsämäki, SAKU T Anttila, HUTTUNEN J Markus, 2005. A feasible method for fractional snow cover mapping in boreal zone based on a reflectance model [J]. Remote Sensing of Environment, 95: 77- 95.

SOLBERG R, HILTBRUNNER D, KOSKINEN J, 1997. Snow algorithms and products-review and recommendations for research and development [R]. Oslo: Norwegian Computihg Center.

VERHOEF W, 1984. Light scattering by leaf layers with application to canopy reflectance modeling: the Sail model [J]. Remote Sensing of Environment, 16: 125- 141.

VIKHAMAR Dagrun, SOLBERG Rune, 2002. Subpixel mapping of snow cover in forests by optical remote sensing [J]. Remote Sensing of Environment, 84: 69- 82.

VIKHAMAR Dagrun, SOLBERG Rune, 2003. Snow-cover mapping in forests by constrained linear spectral unmixing of MODIS data [J]. Remote Sensing of Environment, 88: 309- 323.

WOODCOCK C E, COLLINS J B, JAKABHAZY V D, 1997. Inversion of the Li-Strahler canopy reflectance model for mapping forest structure [J]. IEEE Transactions on Geoscience and Remote Sensing, 35: 405- 414.